Chapter V

Microstructure, Structural Transformation and Magnetic Properties of 500 ºC Annealed TiO_2 Thin Films under Ar^{2+} Ion Irradiation

5.1 Introduction

Ion irradiation is a unique tool to create post-deposition defects, as by appropriately selecting the ion, energy and fluence. In this chapter, we have studied the effect of 500 keV Ar^{2+} ions (low energy ions) irradiation on TiO_2 thin films deposited through e-beam evaporation technique after annealing at 500 ºC. The ion fluences used in irradiation are, 1×10^{14}, 1×10^{15}, 5×10^{15}, 1×10^{16}, 5×10^{16} ions/cm^2.

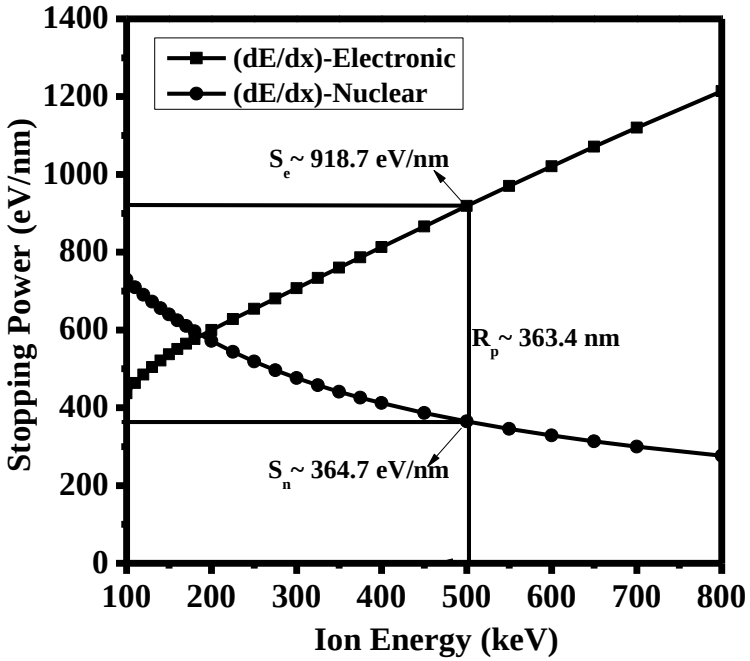

Figure 5.1 *Electronic and nuclear energy loss as a function of energy for argon ion on the TiO_2 target.*

The variation of electronic energy loss (S_e) and nuclear energy loss (S_n) with incident projectile energy (for Ar ion) is shown in Figure 5.1 using SRIM code 2008. It shows 500 keV argon ions, correspond to S_e ~ 918.7 eV/nm, S_n ~ 364.7 eV/ nm, and projected range (R_p) ~ 363.4 nm. Structure and surface morphology of the films are elaborated in Section 5.2. Magnetic properties are discussed in Section 5.3. In Section 5.4, X-ray photoelectron spectroscopic studies are discussed. Conclusions of this chapter are summarized in Section 5.5. The pristine film annealed at 500 ºC for 1 h (deposited on Si) referred as A, and films irradiated with ion fluence, 1×10^{14}, 1×10^{15}, 5×10^{15}, 1×10^{16}, 5×10^{16} ions/cm^2 are referred as B, C, D, E, F, respectively.

5.2 Structure and Surface Morphology

In this section, we have presented structural and surface morphology studies carried out by Rutherford's Backscattering (RBS), X-Ray Diffraction (XRD), Raman Spectroscopy and Atomic Force Microscopy (AFM).

5.2.1 Rutherford's Backscattering

Figure 5.2 depicts the RBS spectra of pristine film, film irradiated with 1×10^{14} ions/cm^2 and 5×10^{16} ions/cm^2. Besides Ti, Si and O, no other elements have been detected from the RBS spectra in either pristine or irradiated films. Thickness of the film obtained from the width of Ti curve is around 360 nm. As the film thickness matches with the projectile range, one may expect the defects created on the surface of the film as well as on Si substrate.

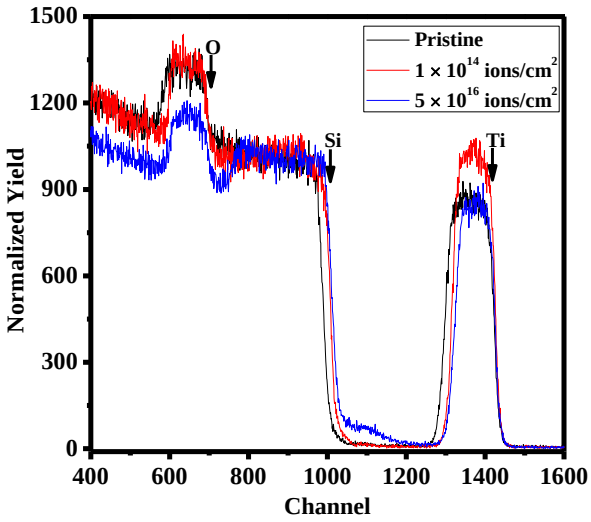

Figure 5.2 *RBS spectra of TiO_2 thin films indicating Ti, Si and O edges.*

5.2.2 X-Ray Diffraction and Raman Spectroscopy

Irradiating TiO_2 thin films with 500 keV Ar^{2+} ions, we have studied structural evolution and post irradiation defects induced damage. Figure 5.3 (a) depicts the glancing angle X-ray diffraction (GAXRD) patterns of the films A to F. Pristine film, A, is crystalline in nature showing diffraction peaks at 25.33º, 37.91º corresponding to (101), (004) of anatase phase of TiO_2 (JCPDS PDF# 894921). After irradiating with the ion fluence of 1×10^{14} ions/cm^2 (B), 1×10^{15} ions/cm^2 (C), 5×10^{15} ions/cm^2 (D) and 1×10^{16} ions/cm^2 (E), film shows amorphous nature. Film after irradiating with ion fluence 5×10^{16} ions/cm^2 (F) exhibits crystalline nature. The diffraction peaks in film F, are at 30.33º and 42.96º which correspond to (211) and (410) of brookite phase of TiO_2 (JCPDS PDF# 761934). Thus, one may note that anatase phase of TiO_2 transforms to brookite phase through an intermediate amorphous phase with increasing fluence. Raman measurement is further carried out to confirm the anatase to brookite phase transformation (Figure 5.3 (b)). Raman peak at 143

cm^{-1} and 521 cm^{-1} observed in pristine film correspond to E_g band of anatase TiO_2 and Si respectively. No peak found in film B after irradiating with 1×10^{14} ions/cm^2, supports the XRD results. At 5×10^{16} ions/cm^2, a band at 149 cm^{-1} is observed which almost matches with the brookite phase reported by Hu et al. (2003)b. In addition, we observe a peak at 521 cm^{-1} corresponding to Si substrate which is suppressed. Therefore, one may note that low energy ion irradiation, not only involves with a phase transformation from anatase to brookite but also modifies the surface of the substrate, because, the projected range (R_p) of irradiated ion is slightly higher than the thickness of the film. In our previous results, 100 MeV, Ag ion irradiation in Co-doped TiO_2 films demonstrates a decrease in crystallinity with ion fluence and finally become, amorphous in nature [Mohanty et al. (2014)b]. Among three existing phases of TiO_2 such as anatase, brookite and rutile, it may be mentioned that while anatase and rutile are most common phases observed in TiO_2 depending on size,

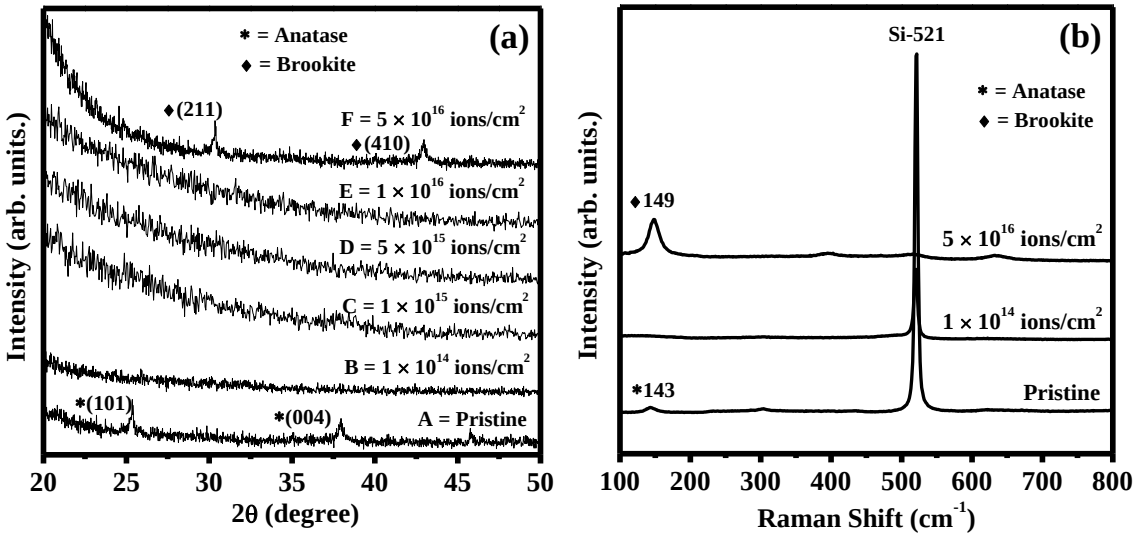

Figure 5.3 *(a) GAXRD pattern of TiO_2 thin films annealed in O_2 environment at 500 ºC before and after irradiation with 500 keV Ar^{2+} ions and (b) Raman spectra of TiO_2 thin films before and after irradiating with 500 keV Ar ion.*

annealing temperature and pH of precipitation, brookite phase is occasionally observed in TiO_2. Moret et al. (2000), obtain brookite phase of TiO_2 thin film by pulsed laser deposition in oxygen environment. Irradiation of 200 MeV Ag ion in TiO_2 thin film deposited through spin coating, Rath et al. (2009)b, observe transformation from anatase to rutile phase. Thakur et al. (2011)a, show phase transition from anatase to mixed brookite and rutile phase in the TiO_2 film deposited through RF sputtering after irradiating with 200 MeV Ag ion. No such report so far show stable brookite phase of TiO_2 thin film after irradiating with either low or high energetic ions.

5.2.3 Atomic Force Microscopy

We have studied the surface roughness and grain structure elaborately using atomic force microscopy. Figure 5.4 depicts the 2D surface topography and 3D representation of the films A, B and F. The scan surface area is equal to1 μm × 1 μm. Topography of the films indicate uniform and smooth surface. From 3D representation, one may note that all the films show nano-hillock like structure distributed uniformly over the film surface which is similar to our previous report [Mohanty et al. (2014)b]. Surface of pristine film is almost smooth whereas the film irradiated with ion fluence 1×10^{14} ions/cm^2 shows surface cracks. While at a fluence of 1×10^{14} ions/cm^2, different size of hillock structures are randomly distributed, at a fluence of 5×10^{16} ions/cm^2, hillocks become bigger in size. Figure 5.5 shows the roughness histogram. The roughness histogram**,** calculated from surface topography analysis indicates a narrow distribution with high roughness in pristine film (A), whereas a narrow distribution with reduced roughness observed in film F. The surface roughness quantitatively expressed by the root-mean-square roughness (Rrms) for the films A, B and F is found to be 2.08, 3.5 and 1.7 nm respectively. The high R_{rms} observed in film

B could be due to amorphous nature. Figure 5.6 depicts typical 2D and 3D representation of grain structure with grain size distribution in film A and F. The nanostructured thin films,

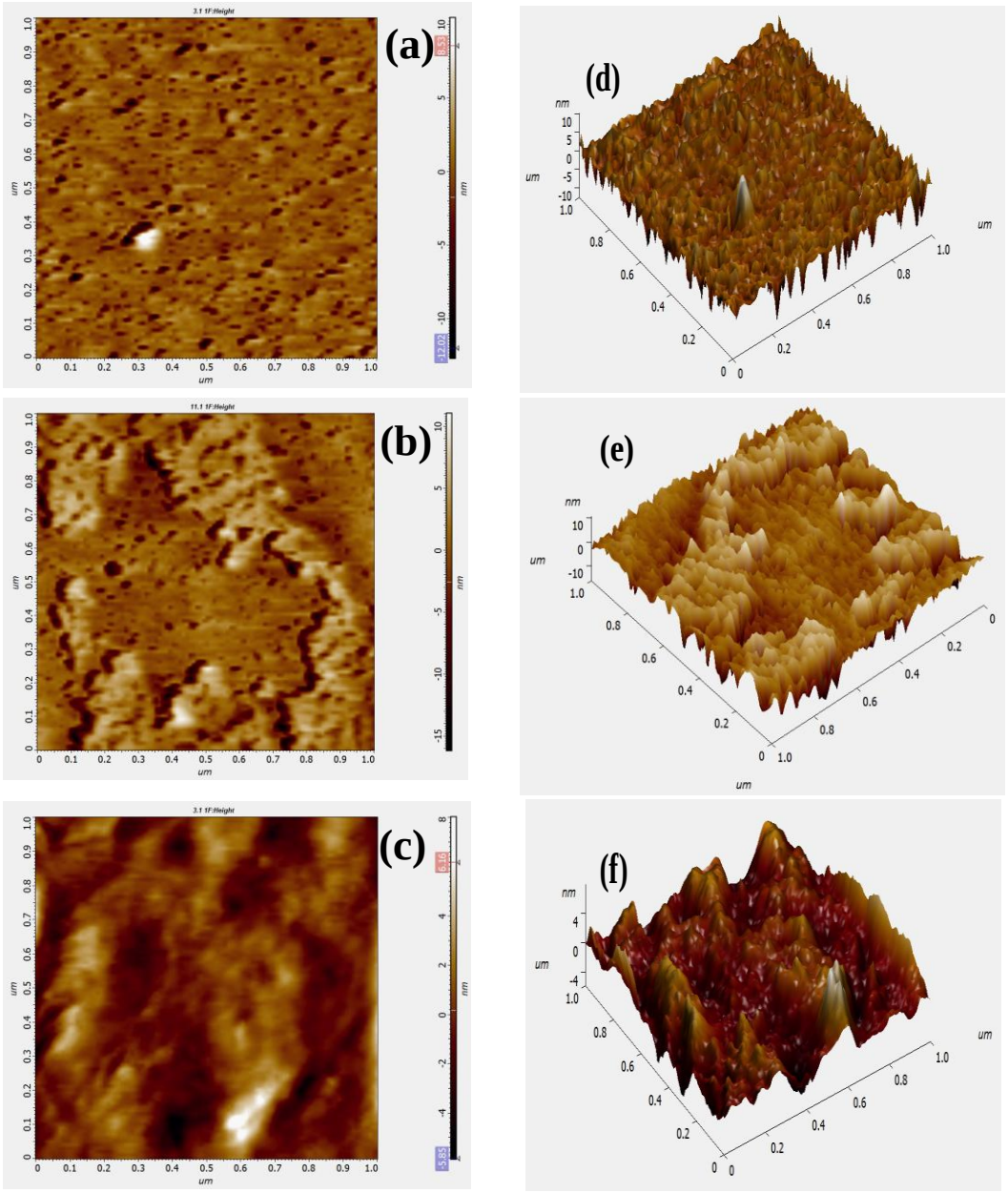

Figure 5.4 *SPM image for topography of TiO_2 thin films A, B, F are (a), (b) and (c), respectively; (d), (e) and (f) depict the 3D representation of the respective films.*

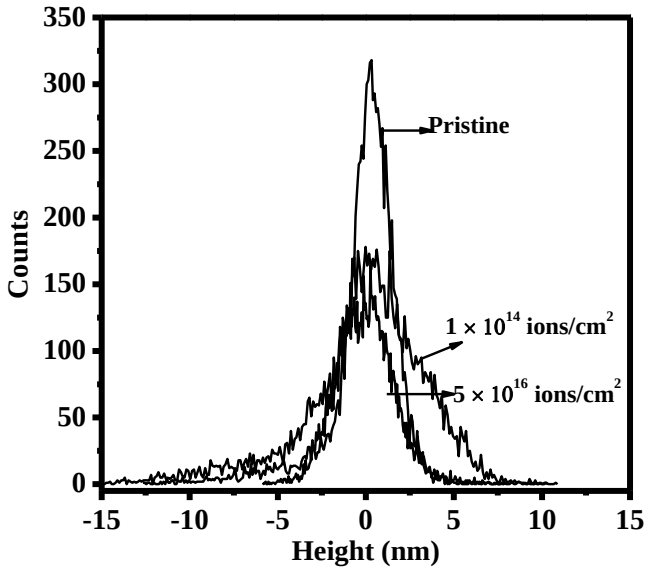

Figure 5.5 *Roughness histograms of TiO_2 thin films before and after irradiating with 500 keV $Ar2^+$ ion.*

both pristine and irradiated one, show a dense granular microstructure with discrete grain boundary. The grain size distributions are fitted to a lognormal function, yielding an average grain size and grain distribution shown in Figure 5.6 (e) and (f). Grain analysis, demonstrates the grain size in pristine film as 22.6 nm with size distribution of 10 to 50 nm; whereas after irradiating with 5×10^{16} ions/cm^2, the average grain size is increased to 84.5 nm showing a broad size distribution from 30 to 200 nm. Grain size distribution shifting towards higher particle size with increase in irradiation fluence indicates grain growth supported by Rath et al. (2011). This could be due to coalescence and coarsening of grains. The TiO_2 films irradiated with 1×10^{14} ions/cm^2, shows amorphous nature which again crystallized in brookite phase after irradiating with 5×10^{16} ions/cm^2. The increase in grain size with increase in grain size distribution thus involves both crystalline phase as well as growth of the particles. Evolution of nanoparticles under ion irradiation is expected to be

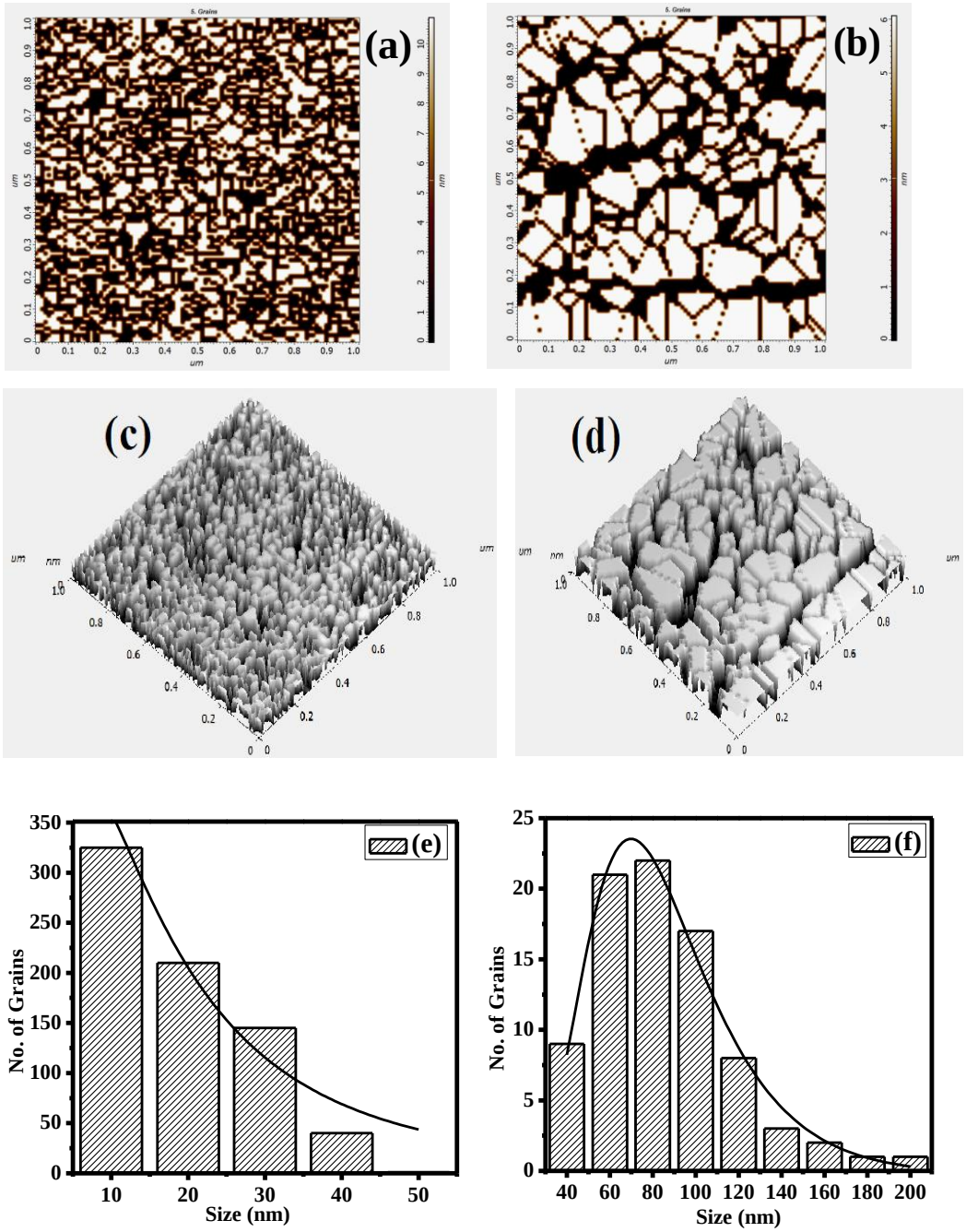

Figure 5.6 *SPM image of TiO_2 thin films with grain structure of films A and F are (a), (b) respectively; (c), (d) depict the 3D representation of the respective films and (e), (f) represents grain size distribution.*

governed by the confinement of a high density of energy deposited by 500 keV ions. With irradiation, the local thermalization in the electronic system is ~10^{-4} sec [Rath et al. (2009)b]. Energy deposited on the electrons are then transformed to the lattice by electron-phonon coupling in a time of 10^{-4} and 10^{-12} sec, which increases the lattice temperature to such an extent that transient temperature rise leads to amorphisation in a crystalline medium as we observe after irradiating with fluence of 1×10^{14} ions/cm^2. The crystalline phase to amorphous phase formation occurs if the melted zone along the ion path is quenched at a rate of 10^{14} ks^{-1}. At higher fluence i.e. 5×10^{16} ions/cm^2, due to the amorphous nature of the film, the heat deposited by the ions is localized and dissipates less heat to the neighboring atom due to low thermal conductivity. The localized region becomes crystallized and particle grows more as observed in film F. The crystalline phase is brookite.

5.3 Magnetic Property

The magnetic properties of these films are determined by carrying out magnetization measurement with varying external magnetic field from 0 to 10 kOe. After removing the diamagnetic contribution of Si substrate, the results are shown in Figure 5.7 (a). All the films show hysteresis with finite coercivity and remanence which is an indication of ferromagnetic behavior. One may note that irrespective of phase and crystallinity, ferromagnetic behavior in all the films retain at room temperature. Figure 5.7 (b) shows the zoomed view of the hysteresis curves. In film A, magnetization saturates at 4 kOe and shows saturation magnetization (M_s) of 8.69 emu/cc, whereas in ion irradiated films B and F, magnetization increases with increase in applied magnetic field and almost saturates at 6 kOe field with saturation magnetization 16.18 and 13.57 emu/cc respectively. Both coercivity and remanance increases with ion fluence. It is surprising to note that even in

amorphous film B, H_c and M_r is also higher than the crystalline film A. Room temperature ferromagnetism (RTFM) in films deposited by e-beam evaporation annealed in Ar and O_2 atmosphere has been reported earlier, where the phase of the films was anatase [Mohanty et al. (2014)a]. Thakur et al. (2011)b, report RTFM in TiO_2 thin films irradiated with Ag ions and phase transformation from anatase to mixed rutile and brookite phase. Ferromagnetism is explained on the basis of distorted TiO_6 octahedra after irradiating with swift heavy ions. Here, we show the RTFM in brookite phase which has not been reported earlier. The unusual appearance of RTFM in diamagnetic substances like TiO_2, HfO_2, In_2O_3 etc. is still not clear [Hong et al. (2007)]. However, it has been demonstrated that RTFM could be due to the contamination caused by the sample holder, impurities in substrate and/or in films, oxygen vacancies or reduction in valency of Ti^{4+} to Ti^{3+} or Ti^{2+} which is magnetic.

5.4 X-Ray Photoelectron Spectroscopy

To further explore the origin of RTFM and the variation in saturation magnetization with ion fluence, we have carried out XPS of films A, B and F. It is an excellent probe to determine the charge state of the cations. In addition, careful analysis of O 1s core level spectra can qualitatively indicate the oxygen vacancy concentration. Consequently, the effect of oxygen vacancy on the valency of Ti can be detected [Hoa et al. (2013) and Santara et al. (2014)]. Figure 5.8 (a) shows the XPS full scan survey of films A, B and F which seems identical and does not show any impurity. To examine further, the O 1s and Ti 2p core levels are scanned. Figure 5.8 (b) depicts the O 1s core level spectra which is asymmetric around the binding energy 530 eV in film A, B and F. The spectra are fitted with two Gaussian peaks, denoted as Oa and Ob using XPS peak4.1 software with Shirley background. While Oa peak is ascribed to the oxygen atoms of bulk TiO_2, the Ob peak is

assigned to the chemisorbed oxygen, organic oxygen contamination and hydroxyl groups on the surface of the film. As the increase in Ob region indicates the increase in oxygen vacancies [Mohanty et al. (2014)a]. We have calculated the area ratio of Ob to Oa, which are found to be 0.97, 2.17 and 1.14 for film A, B and F respectively. Higher is the Ob to Oa area ratio, higher is the oxygen vacancies. Thus, the highest area ratio of Ob to Oa in film B is

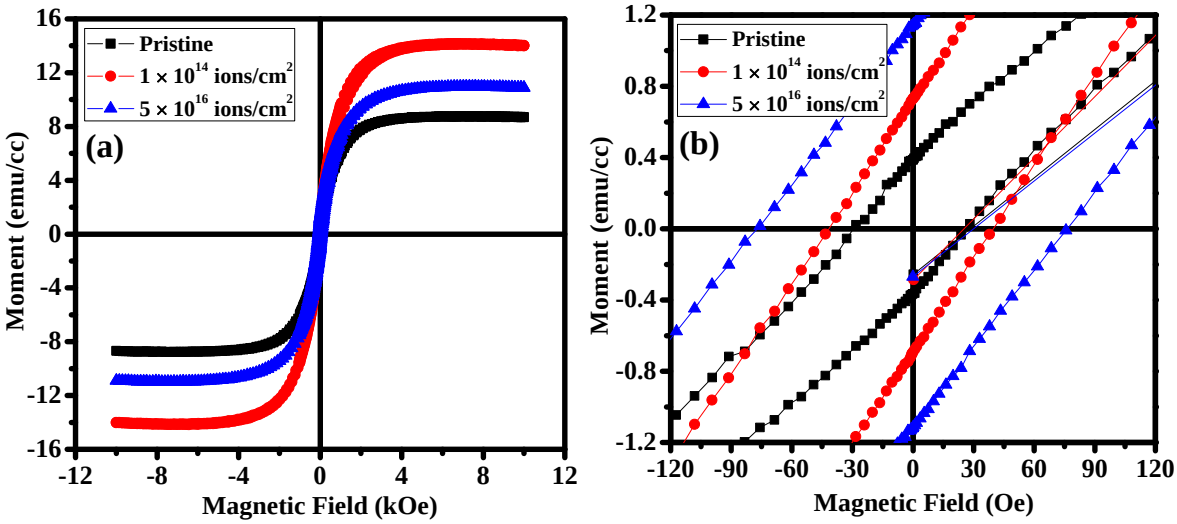

Figure 5.7 *(a) Magnetization as a function of applied magnetic field of films A, B and F, are at 300 K, (b) show the zoomed view of the M–H loops.*

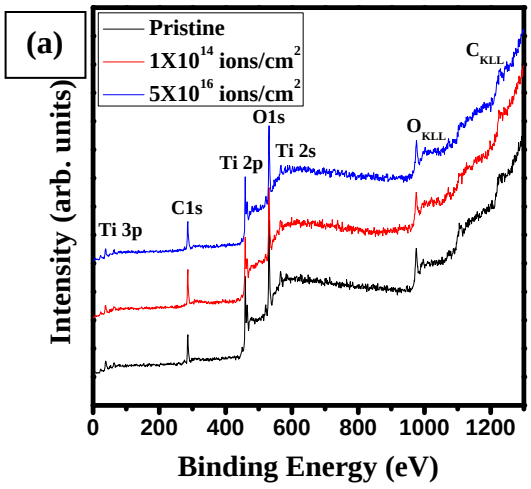

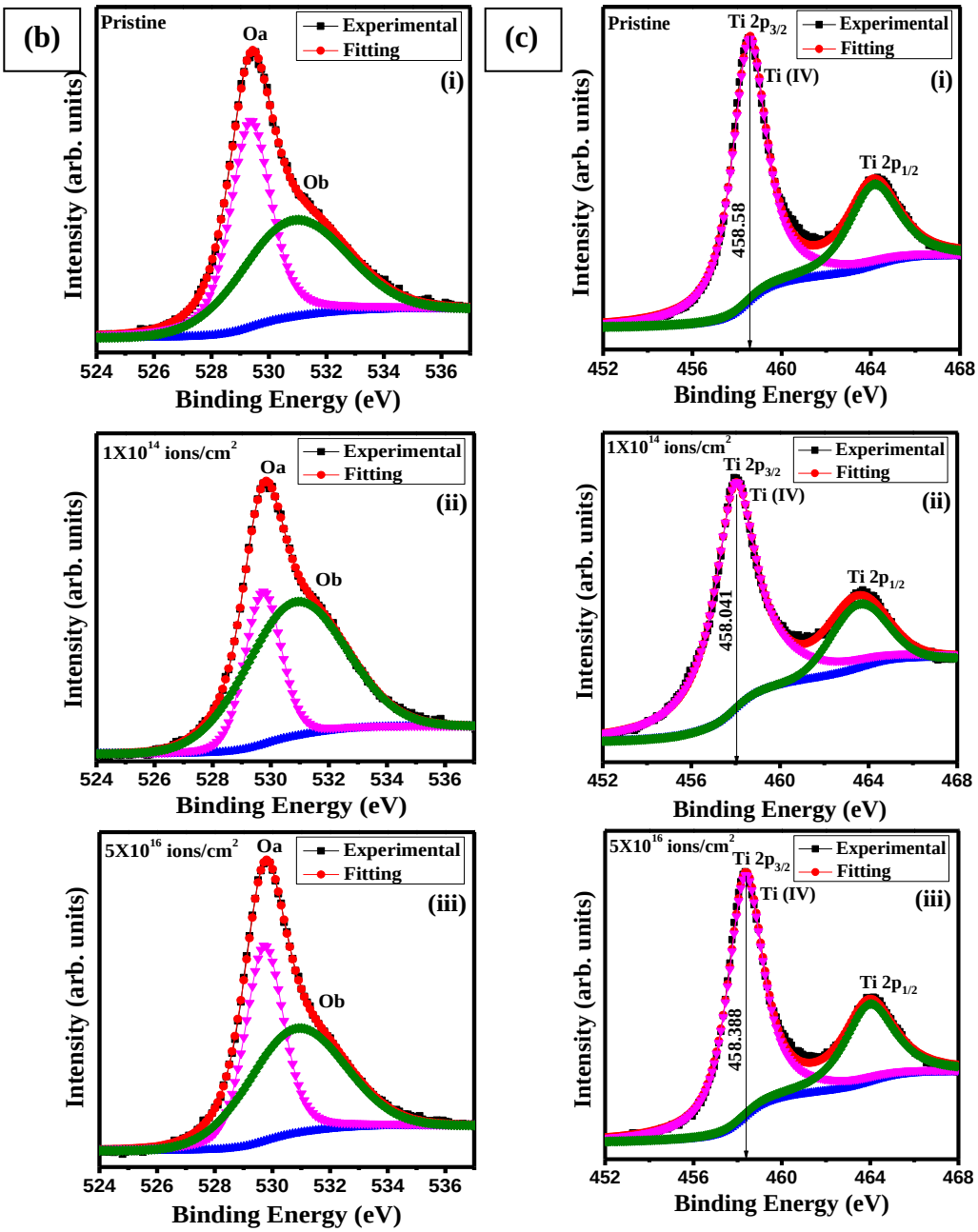

Figure 5.8 *XPS of TiO_2 films A, B and F (a) full survey scan (b) Oxygen 1s core level spectra having Gaussian fitting with Shirley background (c) Ti 2p core level spectra.*

responsible for the high saturation magnetization. In crystalline films reduced Ob to Oa ratio indicating minimum oxygen vacancies and consequently less saturation magnetisation.

Figure 5.8 (c) illustrates the Ti 2p core level spectra. An acceptable fitting is obtained after fitting the Ti $2p_{3/2}$ core level spectra to a single peak. The binding energy for the peak, Ti $2p_{3/2}$ observed around 458 eV confirms the presence of Ti^{4+} valence state which does not change in irradiated films B and F. A careful observation indicates shifting in Ti 2p level towards lower binding energy in film B and F gives an indication of creation of more oxygen vacancies (Figure 5.8 (c) (i), (ii) and (iii)). Sharma et al. (2011) have shown similar shifting in Ti 2p level spectra towards lower binding energy and attribute to oxygen vacancies. Therefore, we have confirmed that RTFM in the present case is due to the oxygen vacancies, which we reported earlier, in Co doped TiO_2 thin films deposited by PLD with and without ion irradiation and undoped TiO_2 thin films deposited by e-beam evaporation technique [Mohanty et al. (2011, 2012, 2013 and 2014)]. Similar evidence have been given by Rumaiz et al (2007), which attribute the magnetism to oxygen vacancies rather than Ti^{3+}/Ti^{2+} cations. Hong et al. (2007) attribute RTFM in In_2O_3, HfO_2 and TiO_2 thin films and assumed that it is due to oxygen vacancy considering their experimental results. Kim et al. (2009) have observed RTFM in both anatase and rutile phases of TiO_2 due to oxygen vacancies. Wei et al. (2009), explain that the oxygen 2p electron plays an important role in the exchange interaction and ferromagnetic ordering.

5.5 Conclusions

TiO_2 thin films deposited by e-beam evaporation technique and annealed at 500 ºC in O_2 environment were irradiated with 500 keV Ar^{2+} ions. Evolution of structure and magnetic properties with ion fluence in thin films were investigated. From GAXRD, it was observed that film annealed at 500 ºC crystallized in anatase phase. After irradiating with Ar^{2+} ions of ion fluence in the range 1×10^{14} to 1×10^{16} ions/cm^2, long range atomic

ordering disappeared and film transformed to amorphous phase. When the film was irradiated with 5×10^{16} ions/cm^2, film again showed crystalline behavior and phase was found to be brookite. Although anatase to rutile phase transformation is an usual phenomenon, the transformation from anatase to brookite phase through intermediate amorphous phase induced by ion irradiation was observed for the first time in TiO_2. Elements Ti, Si and O, were detected from the RBS spectra in either pristine or irradiated films. From SPM, it was found that roughness was more in amorphous films than in the crystalline ones. Although magnetic measurements showed RTFM irrespective of phase and crystallinity, we observed unusually high saturation magnetization in amorphous films than in crystalline ones. The high saturation magnetization was explained on the basis of high oxygen vacancies determined from XPS.